Chinese Journal of Polar Science, Vol. 13, No. 2, 145 - 156, December 2002

Vertical properties of nutrients and oxygen under temperature-salinity structure of the Bering Basin in July 1999

Jin Mingming (金明明)

Laboratory of Ocean Dynamic Processes and Satellite Oceanography, and Laboratory of Submarine Geosciences, Second Institute of Oceanography, SOA, Hangzhou 310012, China

Received June 11, 2001

Abstract The China R/V *Xuelong* went on the first Arctic scientific cruise, and we obtained 271 hydro-chemical samples from 22 deep-sea stations in the Bering Basin in late July, 1999. Here we describe vertical properties of silicate [Si], dissolved inorganic nitrogen [DIN] or [N] (nitrate plus ammonium plus nitrite), phosphate [P] and oxygen [O_2] in seawater under potential temperature-salinity structure. The seasonal stratification in the summer and the water exchanges of the North Pacific Ocean over the Bering Basin resulted in that the four layers of vertical structure with two thermoclines may be found. Vertical [Si] and [N] and [P] profiles show that the nutrients are consumed mainly in ≤50 m and the order of deficient nutrients is [Si] the first, [N] the second and [P] the third. The [N] and [P] increase with depth downward to about 500 m and then both decrease, but the [Si] increases from 150 m to 2000 m or the bottom. In ≥150 m the [O_2] decreases, which is related with both [P] and [N] increasing closely. Seawater [N]:[P] ratios are 6 - 12 in ≤50 m, 10.5 - 14.3 in 100 - 150 m and 11.7 - 15.8 from 300 m to the bottom.

Key words nutrients, oxygen, potential temperature, salinity, Bering Basin, Arctic.

1 Introduction

The Bering Sea is the marginal sea between the Arctic Ocean and North Pacific Ocean. Between the Aleutian Basin and North Pacific, the sea water freely exchanges through the Aleutian Passes and the Near Straits, where the exchange of sea water may go on in a depth of 4.4 km at the Kamchatka Straits (Roden 1995). The tide, wind, ice, and vigorous sea-air energy affected the circulation and the thermohaline structure in the Bering Basin (Cokelet and Stabeno 1997; Roden 1995; Verkhunov and Tkachenko 1992). From 86 satellite-tracked buoys, the mean current velocities from the 1000 m isobath reach 40 cm s^{-1} in the 1986 - 1993 Bering Basin (Stabeno and Reed 1994). When and during polar cold air outbreaks, ice was formed annually in the Bering Sea, with ice edge roughly parallel to the shelf break and reaching its maximum on 60°N in 1999 from the sea ice analysis (National Ice Center 2001).

The privious main chemical observations were made in the deep Bering Sea by the joint

U. S. – Russian investigation during the NOAA *Miller Freeman* cruise in August 1991 (Reed *et al.* 1993), and at the eighteen stations of the Bering Sea near the date line during the R/V *Thomas G. Thomas* cruise, which was considered as a part of Pacific Hydrographic Program of the World Ocean Circulation Experiment (WOCE) in July, 1993 (Roden 1995).

In July and August 1999, the China R/V *Xuelong* made the China first scientific cruise in the Chukchi Sea and the Bering Sea and the South Canada Basin. From 20 to 31 July, at the 22 stations the samples were collected from 271 layers in the Bering Basin distributed the four points: 60.0°N, 179.99°W; 56.0°N, 173.35°E; 55.99°N, 176.00°W and 58.43°N, 176.18°W (Fig. 1). Here we intensively describe the vertical properties of nutrients and dissolved oxygen under potential temperature (θ)-salinity (S) structure.

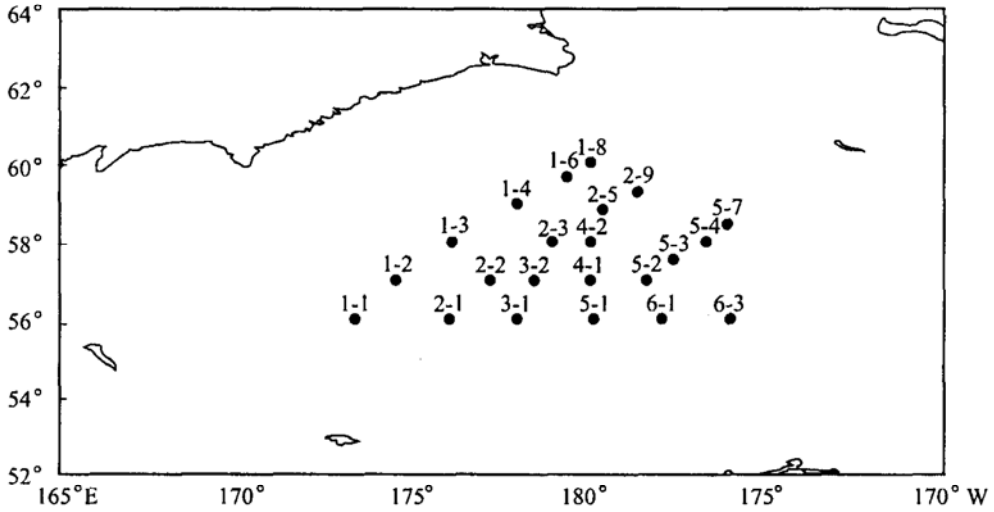

Fig. 1. Station locations in the Bering Basin from 20 to 31 July 1999.

2 Data

The hydrographical properties of seawater were measured by Mark III C (Go Inc, USA) conductive-temperature-depth (CTD) probe. The temperature precision is 0.002°C. The salinity precision is 0.002. The CTD data of 1 dbar pressure bins were processed according to WOCE standards, and potential temperatures (θ) and densities were computed by using the algorithms of the ESO 80 equation of state. The chemical sampling depths from Rosette samplers are 1, 10, 25, 50, 100, 150, 300, 500, 1000, 1500, 2000 m, and/or the bottom, where 3700 m is of the deepest.

Nutrient samples were as soon as possible passed through a cellulose acetate filter of 0.45 μm pore size. Dissolved O_2 is determined by Winkler iodometric titration method. The nutrients were analyzed by manual techniques. Soluble reactive phosphate (P) (Thomson-Bulldis and Karl 1998) and the ammonium (NH_3) plus amino acids are measured by the Strickland-Parsons' methods (1972). Nitrite (NO_2^-) is measured by Grasshoff's method (1999). Dissolved inorganic silicate (Si) is measured at 380 nm by the Sagami Centre method (Sugawara in 1969; Riley and Skirrow 1975; Grasshoff *et al.* 1999), and bias of

salt effects is corrected. The procedure of measuring nitrate (NO_3^-) is based on a method by Chow and Johnstone (1962) with some modification (Jin and Tang 2002). The precisions of the P, NO_3^-, NH_3, NO_2^-, Si and O_2 are 0.01, 0.1, 0.1, 0.02, 0.1 and 0.5 μmol L^{-1} (μM), respectively.

3 Results

3.1 The θ and S structures

Fig. 2a. – d give the θ and S profiles on 20 – 31 of July 1999. There is a four-layers structure with two thermoclines. A top layer in ≤22 m is warm (7.305°C – 8.399°C), low-salinity (<33.13). Then, there is the first plain thermocline. After it a q minimum (0.532°C – 2.325°C) layer of 100 – 120 m thick is found in ≤157 m, where most of salinities change little (33.0 – 33.2) with depth. Then, there are the second reverse thermocline and a halocline of from 33.0 – 33.3 to 33.5 – 33.7. Next is 300 m thick θ maximum (mainly 3.43°C – 3.98 °C) in 200 – 500 m, where salinities continue to increase with depth. The bottom layer is a gradual θ decrease from 3.43°C – 3.58°C at 500 m to 1.31° C at 3700 m, and gradual S increase from 33.92 – 34.12 at 500 m to 34.66 at 3500 m.

The top layer, the θ minimum layer and the second reverse thermocline of the halocline produce the strong V-form in θS structure (Fig. 3). Before the *q* minimum (0.53 – 2.3°C, 33.01 – 33.17 salinity) is a loosely clustered branch. Between the *q* minimum and *q* maximum (3.963°C, 33.55) is the second clustered branch. Beyond 33.73 and < 3.96 °C is the third tightly clustered branch. These indicate that the seawaters under depth of the θ minimum are conservative.

3.2 Vertical oxygen and nutrient profiles

The O_2 equilibrium concentrations at 100 % humidity and 20.95 % O_2 at 1013.25 hPa are calculated by the Weiss equation (UNESCO in 1973, Grasshoff *et al.* 1999). Fig. 4a – 4d show the vertical O_2 concentrations [O_2] and vertical O_2 saturation (%) in the sampling layers. Both are in the same three layers. The first layer is in <200 m, and the main parts have [O_2] (its saturation) from 8.82 mL/L (114.8%) to 6.58 mL/L (87%). All the exceptive under the main parts are at 50 m; they are 6.30 mL/L (84%) at the 6 – 3 station, 5.66 mL/L (72%) at the 1 – 3 station, and 4.92 mL/L (65%) at the 3 – 1 station. The oxycline lies from 5.89 – 7.56 mL/L (77.9 – 98.8%) in 150 – 200 m to 1.52 – 3.22 mL/L (18.8 – 43.78%) in 300 m. Then the second layer of the low O_2 is of < 2.0 mL/L (< 20%) in 300 – 2000 m. In the third layer, O_2 increase slowly from 1.44 mL/L at 2000 m to 2.39 mL/L (18.79 – 30.97%) at 3700 m.

Goldman *et al.* (1979) considered either nitrogen source (NH_4^+ – N, NO_2^- – N, NO_3^- – N, urea-N) or growth rate has no effect on cellular [N]:[P] ratios. Hence, we regarded NO_3^- plus NH_3 plus NO_2^- as dissolved inorganic nitrogen (N). Fig. 5a – 5f are the vertical distributions of silicate concentrations [Si], DIN concentrations [N], and

phosphate concentrations [P] in the sampling layers.

The basic Si structure (Fig. 5a－5b) is as follows. Most of [Si] in ≤25 m is 3.68－40 μM. Then a Si-cline follows. Beneath it there is a layer of 40－70 μM in 50－200 m. Afterwards, a broad Si-cline of 70－160 μM follows from 200 m to 2000 m. Between 2000 m and bottom, there is a little increase of the Si within 10 μM.

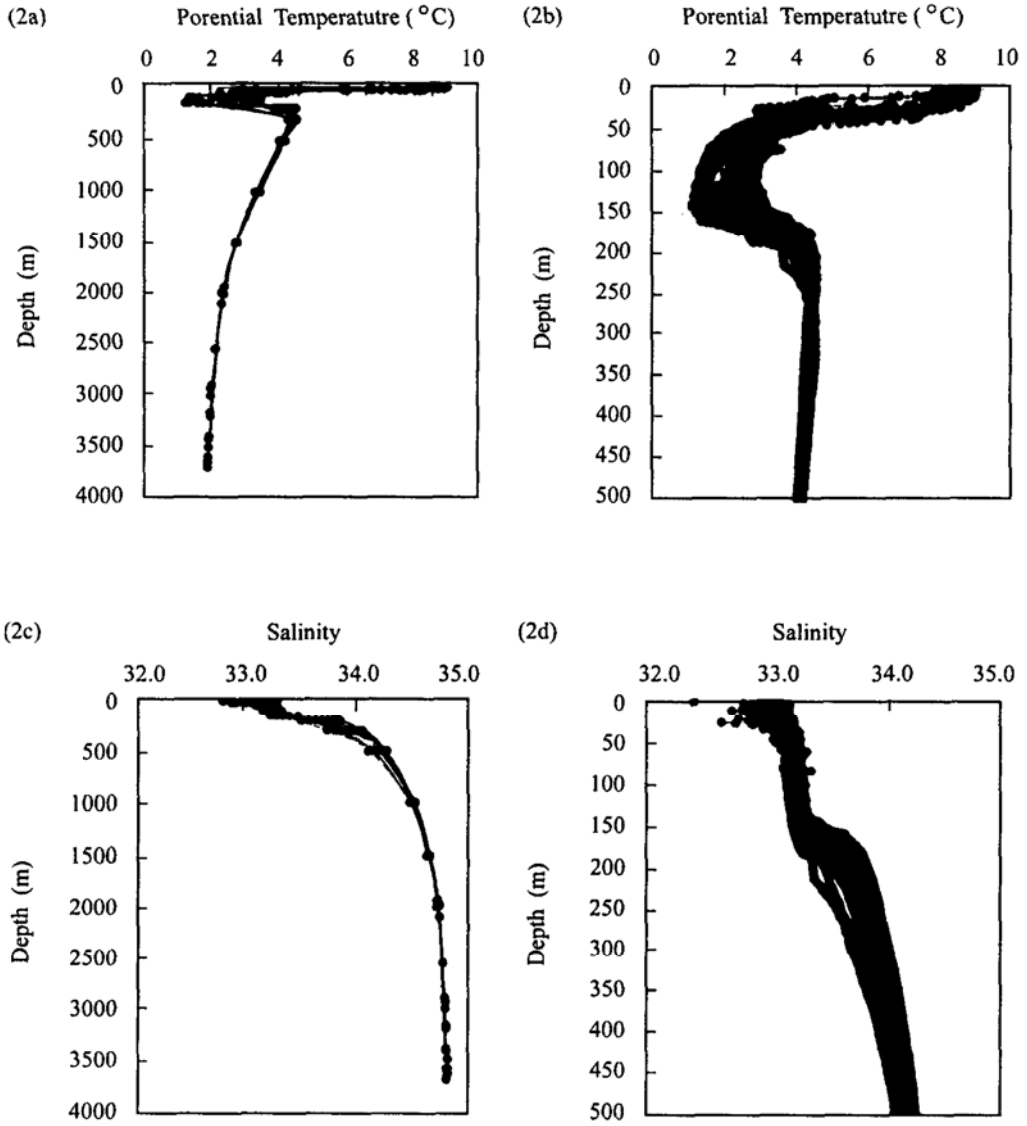

Fig. 2. Vertical potential temperature (θ) profiles (2a) and its details above 500 m (2b), and vertical salinity (S) profiles (2c) and the details above 500 m (2d). Vertical θ and S profiles are drawn by data of the sampling layers with trend lines, but vertical θ and S profiles above 500 m are drawn by the data of 1 dbar pressure bins.

The basic N structure (Fig. 5c－5d) is as follows. Most of [N] in ≤25 m is 6.1－15 μM. Then a N-cline follows, and the [N] reaches 17.4－24 μM at 50 m. Beneath it there is a layer of 20－28 μM from 50 m to 150－200 m. Though the [N] still increases to 40－46 μM in 200－500 m, the [N] decreases or remains to 38－45 μM between 500 m

and the bottom.

The basic P structure (Fig. 5e-5f) is as follows. Most of the [P] in ≤25 m is 0.66 -1.6 μM. Then a P-cline follows, and the [P] reaches 1.74 -2.05 μM at 50 m. Beneath it there is a layer of 2.0 -2.5 μM from 50 m to 150 -200 m. Though the [P] still increases to 3.0 -3.24 μM in 200 -500 m, the [P] decreases to 2.9 -3.1 μM between 500 m and the bottom.

4 Discussion

4.1 The θ maximum layer

In the four-layers θS structure (Fig. 3), heat input from the atmosphere from 1 May (by the sea ice analysis; National Ice Center, 2001) to 31 July 1999 gives the shallow top layer ≤22 m. This 22 m depth is shallower than the 30 m depth of a station in the center of the South Aleutian Basin in July 1993 (Roden 1995). Then, the θ minimum layer of about total 100 m depth is a remnant of the winter mixed layer. The 0.532°C minimum in the North in July 1999 (Fig. 3) is lower than the about 1.6°C in the South in July 1993 (Roden 1995), but the following 3.433 - 3.978°C maximum in the northern Bering basin (Fig. 3) is wider than the 3.6 -3.7°C maximum at the 7 to 13 stations in the southern Bering basin (Roden 1995). In our θS plot, the > 4°C points of the first branch in the northern Bering basin (Fig. 3) are similar to those in the east at the 1 to 6 stations (Roden 1995), and the points of strong V-shaped θ minimum in the northern Bering basin (Fig. 3) are similar to those at the 7 to 13 stations in the southern Bering basin (Roden 1995). And beyond the θ maximum, the θS points both in the Northern (Fig. 3) and in the Southern (Roden 1995) are consistent.

Fig. 2b shows the prominent θ maximum of 3.591°C -3.98°C in 200 -400 m of the 22 stations in the Bering Basin. Cokelet and Stabeno (1997) considered the characteristic, deep, 3.7°C -4.0°C maximum in 200 -400 m in the southeast Bering Sea steming from warm Alaskan Stream. We considered that there is a possibility of other factors. For instance, the θ maximum may come from the waters of the North Pacific Ocean as well. The vertical T and S section just across Kamchatka Straits of 4.4 km depth in August 1991 (Reed *et al.* 1993) agrees with our vertical θ and S distributions (no figure is shown here) in ≤500 m at 3 stations inside of Kamchatka Straits (from 166.3°E, 56.4°N to 164.7°E, 55.7°N) on 31 August 1999. However, we noticed that the 150 μM of [Si] at 500 m of Reed *et al.* (1993) is higher than the 121 -131 μM at 500 m of our 3 stations near Kamchatka Straits (No data was shown here), and higher than the 110 -126 μM at 500 m of our 22 stations (Fig. 5b). More directly, the T and S and density sections along the date line (Fig. 3; Roden, 1995) show the North Pacific seawater in ≤1500 m enters the Bering Sea through Amchitka Pass. And the 100 μM of [Si] at 250 m of North Pacific declines in wavelike way to 500 m of the five station (Fig. 5; Roden 1995). So the whole θ maximum layer and the plain nutricline below the θ minimum are contributed partly by the warm Alaskan Stream, partly by the warm North Pacific seawater, or partly by temperature increase from microbe decomposed soft parts of biogenic matter (4.2 subsection below).

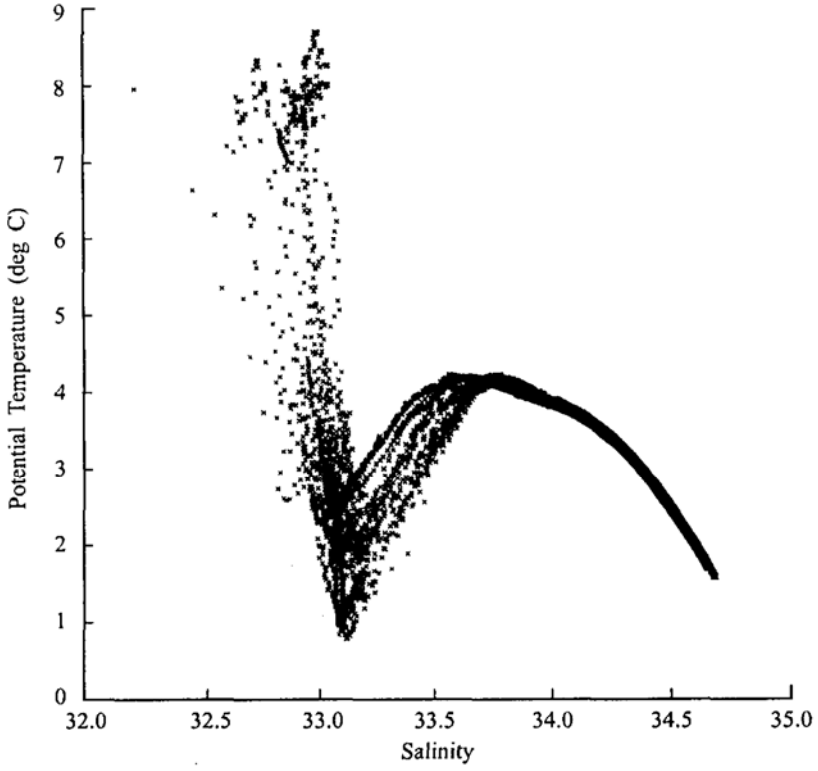

Fig. 3. The θS structure according to the data of 1 dbar pressure bins.

4.2 *Correlation between [Si], [P], [N] and [O_2] in 150 - 300 m*

From Fig. 4b, 4d, 5b, 5d, and 5f, we saw that while the oxygen decreases in 150 - 300 m, the nutrients increase. The calculations of concentrations all by μM unit give [Si] = -0.2076 [O_2] + 12.11 (correlation coefficient $R^2 = 0.9341$, n = 79) in 150 - 500 m layers (Fig. 6a). And the [P] is equal to -0.0039 [O_2] + 3.3375 ($R^2 = 0.9572$, n = 155) at ≥150 m (Fig. 6b). The [N] is equal to -0.0693 [O_2] + 47.142 ($R^2 = 0.9007$, n = 155) at ≥150 m (Fig. 6c). The [NO_3^-] is equal to -0.0694 [O_2] + 47.091 ($R^2 = 0.9027$, n = 155) at >150 m (Fig. 6d). The increasing [Si] comes from dissolution of hard parts of diatoms, while increasing P and N are from dissolution of soft parts of biogenic matter (Jones and Anderson, 1986). The [P] and [NO_3^-] have > 0.9 correlativity with [O_2] in ≥150 m. Every 1 μM [P] and 16 μM [NO_3^-] releases should consume 150 μM [O_2] (Anderson 1995). The process released the heat that would give part contribution to the θ maximum layer. Certainly, two water layers or two water masses may produce the oxycline directly. So we consider a question: how many parts of [O_2] decrease here account for microbe decomposed soft parts of biogenic matter.

4.3 *Nutrient ratios*

From the [Si] and [N] measured, vertical [Si]:[N] profiles (Fig. 7a) are 0.39 - 2.79 in ≤25 m and 1.90 - 2.97 in 50 - 150 m. The [Si] versus [N] plot in ≤150 m

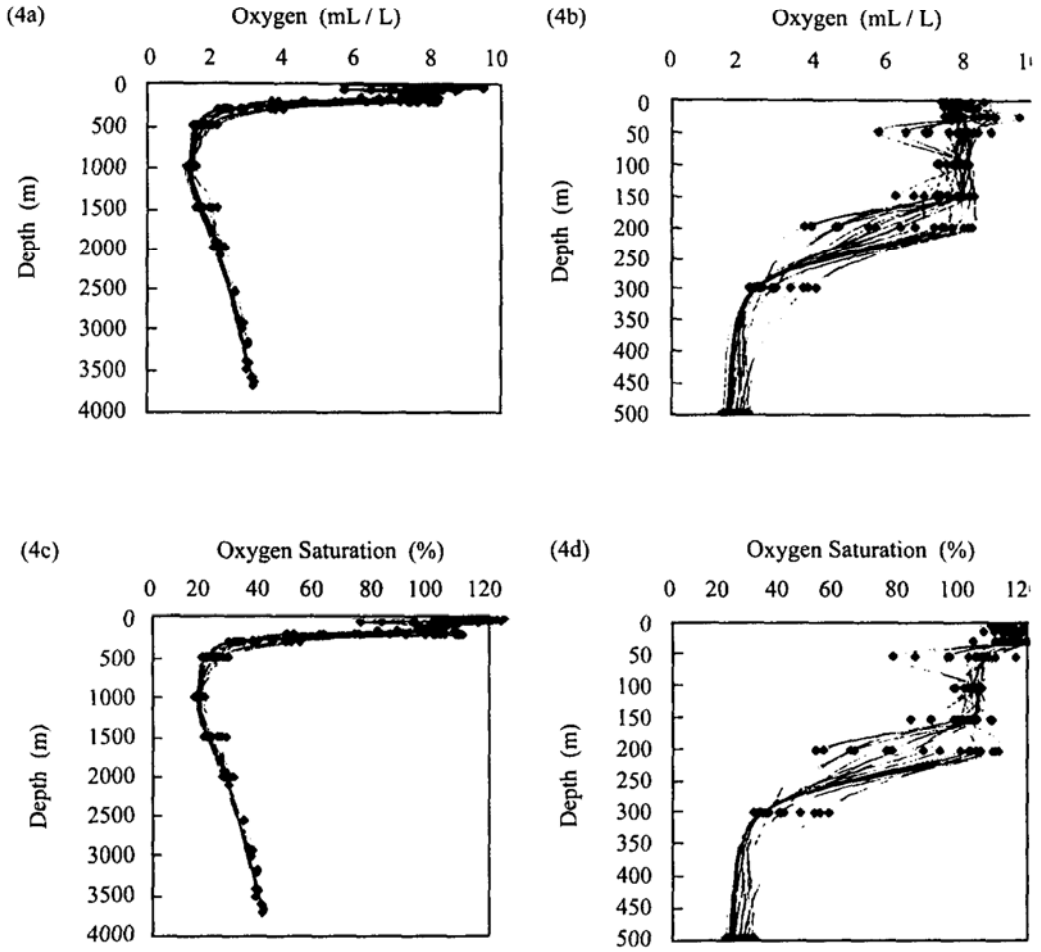

Fig. 4. Vertical oxygen profiles (4a) and its details above 500 m (4b), vertical oxygen saturation profiles (4c) and its details above 500 m (4d).

layers (Fig. 7b) gives regression equation, [Si] = 2.9287 [N] −13.149 (R^2 = 0.9194, n = 131). The 2.9: 1 slope implies trend of [Si]: [N] in 50−150 m. And −13.149 μM indicates [Si] would be depleted moderately before [N] run-out. The −13.149 μM also indicates the about half stations in ≤25 m (Fig. 5b) is lacking in Si relative to N. In contrast, the particulate [Si]: [N] of the surface water in the South of Kerguelen Island (49°39′S, 69°E) of Antarctic Ocean is 2.35: 1 (n = 19), and that in the East of Kerguelen Island is 1.59: 1 (n = 8) (Copin-Montegut and Copin-Montegut 1978).

Vertical [Si]: [P] profiles are 3.3−26.1 in ≤25 m, and 19.3−33.9 in 50−150 m (Fig. 7c). Meantime, Fig. 7d shows [Si] = 39.966 [P] −25.054 (R^2 = 0.895, n = 131) in ≤150 m layers. The 40: 1 slope implies trend of [Si]: [P] in 50−150 m. And −25.054 μM indicates [Si] would be depleted greatly before [P] run - out. The −25.054 μM also indicates most of stations in ≤25 m (Fig. 7a) are lacking in Si relative to P. In contrast, average [Si]: [P] ratio of particles in surface water in the South of Kerguelen Island is 1438: 57.6 = 25: 1 (n = 19) from 4 to 16 April 1974 (Copin-Montegut and Copin-Montegut 1978).

The vertical [N]: [P] profiles (Fig. 7e) are 6−12 in ≤50 m, 10.5−14.3 in 100

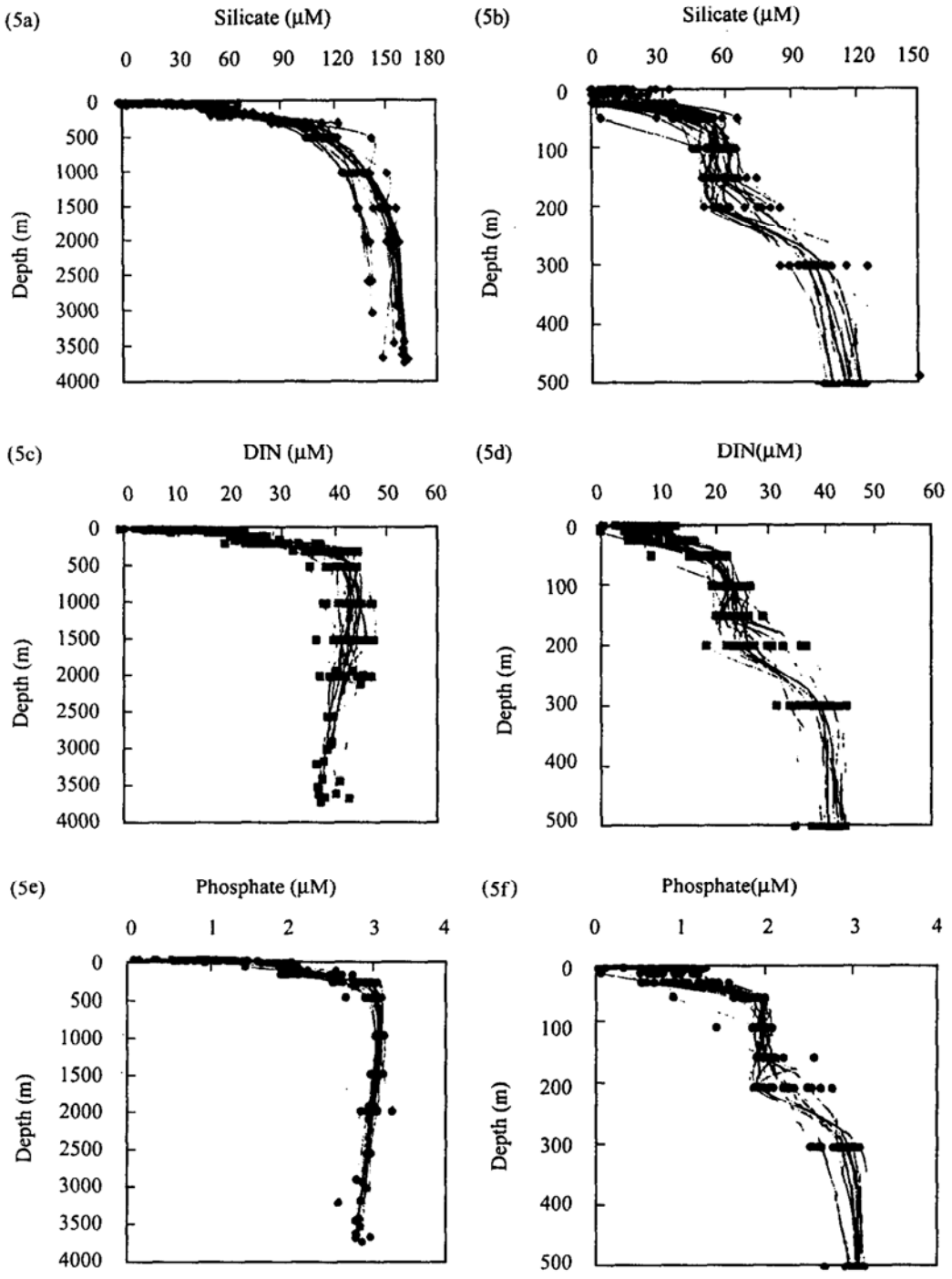

Fig. 5. Vertical silicate profiles (5a) and its details above 500 m (5b), vertical DIN profiles (5c) and its details above 500 m (5d), and vertical phosphate profiles (5e) and its details above 500 m (5f).

−150 m, and 11.7 −15.8 from 300 m to the bottom. The [N] versus [P] plot in 1 −3700 m layers (Fig. 7f) gives [N] = 16.052 [P] −7.2935 (R^2 = 0.969, n =271). The slope follows typical Redfield ratio [N]: [P] = 16: 1, and implies trend of [N]: [P] in > 50 m. And the −7.2935 μM indicates [N] (mainly [NO_3^-]) run-out before [P], just as the phosphate in lakes has the < 10 min turnover times (Hudson *et al.* 2000). The

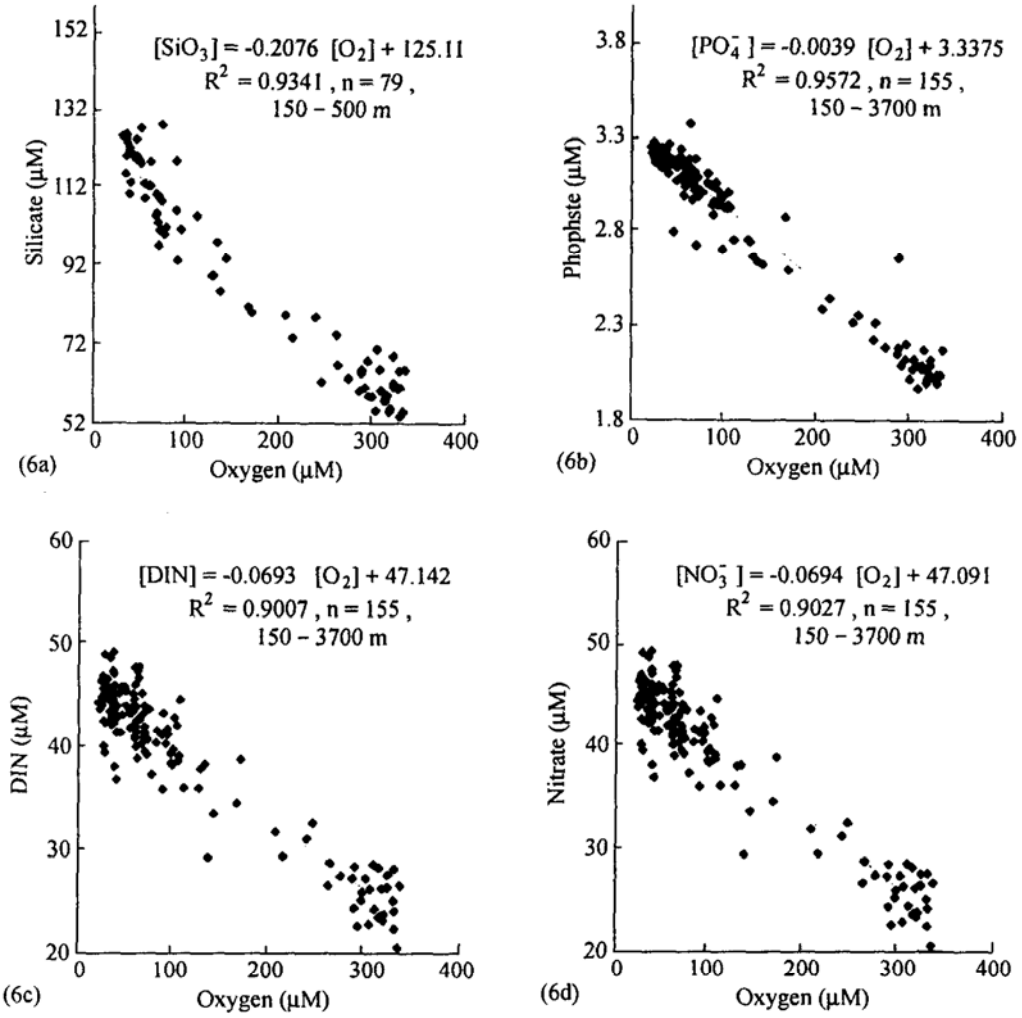

Fig. 6. Silicate (6a) and phosphate (6b) and dissolved inorganic N (6c) and nitrate (6d) versus oxygen plot.

-7.2935 μM also indicates that the few stations in ≤25 m (Fig. 7a) are lacking in N relative to P. The GEOSECS global data in surface water show the $[NO_3^-]$: [P] ≈15: 1 with a small [P] residue as well (Tyrrell 1999). Thus in the upper 25 m of the Bering Basin, most of 22 stations are in lacking Si and few of them in N.

5 Summary

In July 1999, observations of 22 stations made in the Bering Basin show the four layers structures with two thermoclines. A top layer ≤22 m is warm, low-salinity. Then there is the first plain thermocline. Beneath it a θ minimum layer of 100 - 120 m thick is found in 80 - 157 m. The following is the second counter thermocline. In the 200 - 500 m there is about 300-m thick θ maximum. The bottom layer is a gradual θ convergence in 500 - 3700 m. The whole θ maximum layer with plain nutricline below the θ minimum is contributed partly by the warm Alaskan Stream, or partly by the warm North Pacific seawater, or partly

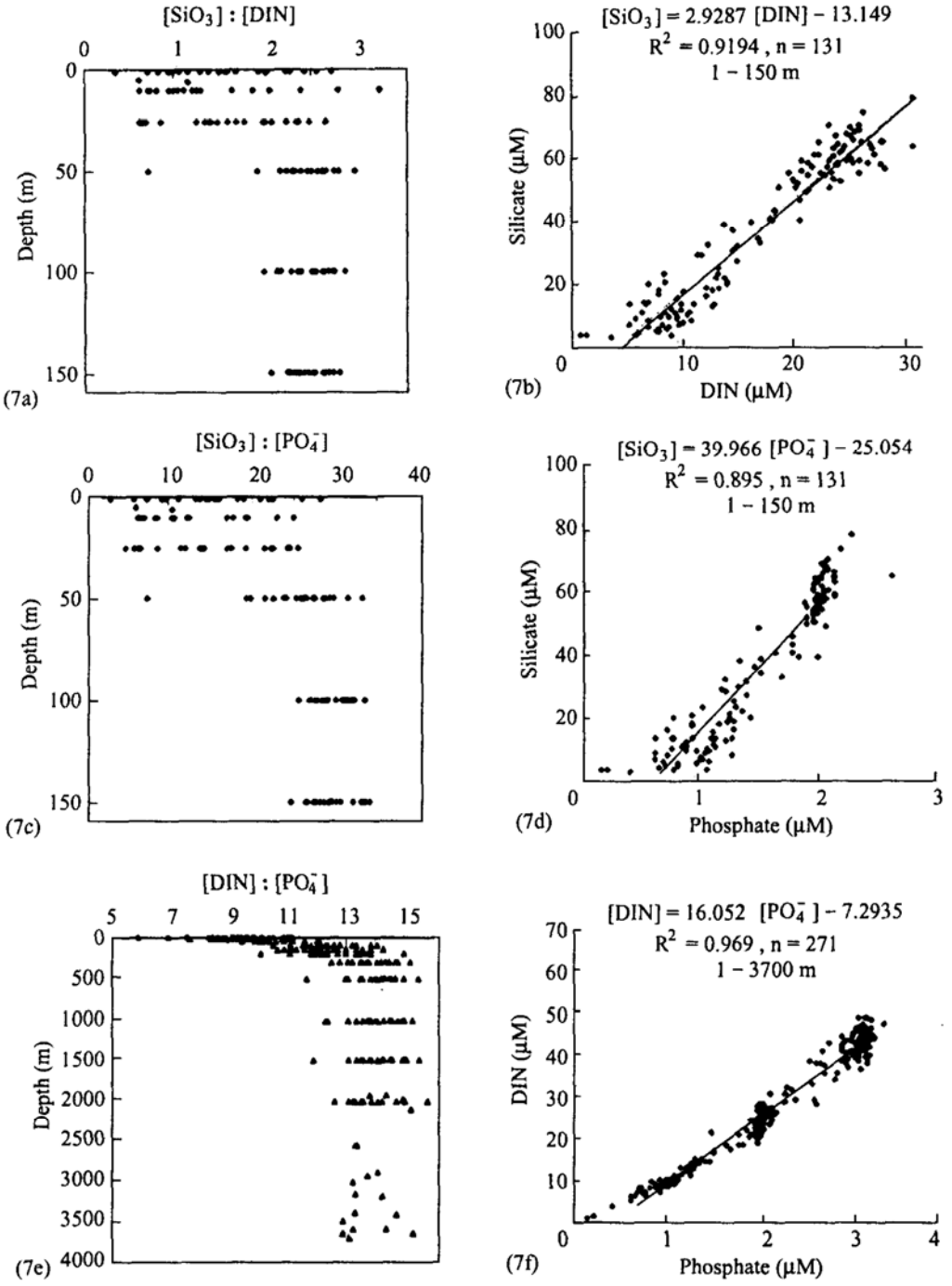

Fig. 7. Vertical [Si]: [N] profiles (7a) and silicate versus nitrogen plot (7b); vertical [Si]: [P] profiles (7c) and silicate versus phosphate plot (7d); vertical [N]: [P] profiles (7e) and nitrogen versus phosphate plot (7f).

by the temperature increase from microbe decomposed soft parts of biogenic matter.

The minimum residue of nutrients in ≤10 m is 3.68 μM of silicate, 1.13 μM of dissolved inorganic nitrogen and 0.19 μM of phosphate. The [Si]: [N] ratios are 0.39 – 2.79 in ≤25 m and 1.90 – 2.97 in 50 – 150 m. The [Si]: [P] ratios are 3.3 – 26.1 in ≤

25 m and 19.3 – 33.9 in 50 – 150 m. The [N]: [P] ratios are 6 – 12 in ≤50 m, 10.5 – 14.3 in 100 – 150 m and 11.7 – 15.8 from 300 m to the bottom. In ≥150 m, the [O_2] decrease and both [P] and [N] increase are due to two-layer mixing or partly due to degradation of biogenic matter. From plots of [Si] versus [N], [Si] versus [P], and [N] versus [P], an order of deficient nutrients is Si the first, N the second and P the third.

Data Disposition The nutrients and oxygen data used in this work will be archived in web address: http://www.chinare.org.cn.

Acknowledgments The author is indebted to the scientific investigation team, Chief Scientist Chen Li-qi, and crew of the R/V *Xuelong*, Captain Yuan Shao-hong; especially to Lu Yong who measured silicate, phosphate and most of dissolved oxygen; and to Gao Guoping of Ocean University of Qingdao who processed the CTD data of 1 dbar pressure bins and computed potential temperature-density data. The author also thanks Dong Zhaoqian, Qin Weijia, Zhao Jinping, Chen Bo, Chen Min, Wang Weiqian, Lin Yi'an and Chen Jianfang for their help. This work was supported by the 1999 China First Arctic Scientific Investigation, and by the ecological 973 Program of China (G1999043704).

References

Anderson L (1995): On the hydrogen and oxygen content of marine phytoplankton. Deep-Sea Research I, 42 (9) 1675 – 1680.

Chow TJ, Johnstone MS (1962): Determination of nitrate in sea water. Analytica Chimica Acta, 27: 441 – 446.

Cokelet ED, Stabeno PJ (1997): Mooring observations of the thermal structure, salinity, and currents in the SE Bering Sea Basin. Journal of Geophysical Research, 102 (C10): 22947 – 22964.

Copin – Montegut C, Copin – Montegut G (1978): The chemistry of particulate matter from the south Indian and Antarctic oceans. Deep – Sea Research I, 25: 911 – 931.

Goldman JC, McCarthy JJ, Peavey DG(1979): Growth rate influence on the chemical composition of phytoplankton in oceanic waters, Nature, 279: 210 – 215.

Grasshoff K, Kremling K, Ehrhardt M (1999): Methods of Seawater Analysis, Third, completely revised and extended edition. Wiley – VCH, Weinheim, 77 – 89; 160; 165 – 167; 177 – 179; 193 – 198.

Hudson JJ, Taylor WD, Schindler DW (2000): Phosphate concentrations in lakes. Nature, 406: 54 – 56.

Jin MM, Tang RY (2002): Nitrate concentration in seawater by zinc cadmium reduction method (in Chinese). Marine Environmental Science, 21 (2): 50 – 56.

Jones EP, Anderson LG(1986): On the origin of the chemical properties of the Arctic Ocean halocline. Journal of Geophysical Research, 91 (C9): 10759 – 10767.

National Ice Center (2001): http:// www.natice.noaa.gov/pub/west_arctic/Bering_Sea/bering_sea_west/1999/.

Reed RK, Khen GV, Stabeno PJ, Verkhunov AV (1993): Water properties and flow over the deep Bering Sea basin, summer 1991. Deep – Sea Research I, 40: 2325 – 2334.

Riley JP, Skirrow G (1975): Chemical oceanography, 2nd Edition, Vol. 3, London: Academic Press, 427 – 431.

Roden GI (1995): Aleutian Basin of the Bering Sea: Thermohaline, oxygen, nutrient, and current structure in July 1993. Journal of Geophysical Research, 100 (C7): 13539 – 13554.

Stabeno PJ, Reed RK (1994): Circulation in the Bering Sea Basin observed by satellite-tracked drifters: 1986 – 1993. Journal of Physical Oceanography, 24: 848 – 854.

Strickland JDH, Parsons TR (1972): A Practical Handbook of Seawater Analysis. Fisheries Research Board of

Canada, Ottawa, 21 - 26; 49 - 52; 77 - 80; 81 - 85.

Thomson-Bulldis A, Karl D(1998): Application of a novel method for phosphorus determinations in the oligotrophic North Pacific Ocean. Limnology and Oceanography, 43: 1565 - 1577.

Tyrrell T (1999): The relative influences of nitrogen and phosphorus on oceanic primary production, 400: 525 - 531.

Verkhunov AV, Tkachenko YY (1992): Recent observations of variability in the western Bering Sea current system. Journal of Geophysical Research, 97 (C9): 14369 - 14376.